

## DEVELOPMENT OF A UNIT CELL MODEL TO SIMULATE THE SURFACE DURING THE THERMOFORMING PROCESS

K. Hildebrandt<sup>1\*</sup>, P. Mitschang<sup>1</sup>, D. Schommer<sup>1</sup>

<sup>1</sup>Institut für Verbundwerkstoffe GmbH, Erwin-Schrödinger-Str. 58, 67663 Kaiserslautern, Germany

\*Klaus.hildebrandt@ivw.uni-kl.de

**Keywords:** simulation, surface waviness, thermoforming

### Abstract

*This study concerns the simulation of the surface quality of continuous fiber-reinforced thermoplastic composites. Therefore, a unit cell based on a twill 2/2 fabric was created using the TexGen software. The geometry data were generated from composite cross-sections using light microscopy. The FE-simulation was done using the tool LS Dyna<sup>®</sup>. Geometric models with a matrix rich surface area were created to evaluate its effect on the surface properties. A thickening matrix layer was found to lower the waviness. To investigate nesting effects various displacement configurations were simulated by shifting the fabric layer below the surface layer in x and x-y direction. The layer alignment strongly influences the surface waviness and should therefore be considered in the evaluation of simulations.*

### 1 Introduction

#### 1.1 Organic sheets and obstacles in visible applications

Thermoplastic continuous fiber-reinforced composites (organic sheets) gain more and more importance within different industries such as aerospace, aircraft, and electronics, as well as in automotive applications. Organic sheets typically are manufactured using fabric reinforcements which lead to fiber volume contents typically around 50 % [1-3]. Having an excellent weight to performance ratio they are used as structural and semi-structural components e.g. as bumper beams in cars or leading edges in aircrafts. However, when it comes to applications where the appearance is of utmost importance organic sheets often do not fulfill the required criteria. This mainly is due to different coefficients of thermal expansion (CTE) of matrix and reinforcement and their inhomogeneous distribution within the composite (Fig. 1), which leads to visible surface waviness.

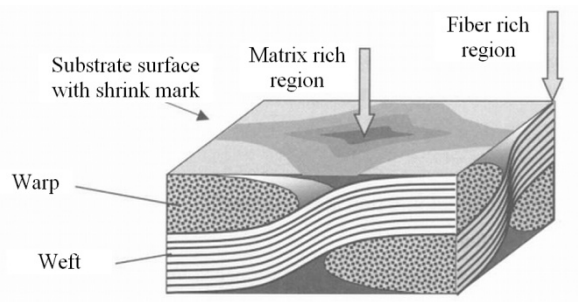


**Figure 1:** Inhomogeneous distribution of fibers and matrix lead to surface waviness.

#### 1.2 State of the art in surface simulation

Therefore, the prediction of surface properties is desired to reduce time and money intensive testing. Several groups started to simulate the surface structure of fiber-reinforced composites in the past years. Blinzler focused on the influence of different thermoplastic matrix systems. In particular he proved that semi-crystalline and amorphous matrices lead to different surface waviness due to their aberrant CTE and the absence of crystalline shrinkage for amorphous polymers (Fig. 2) [4].

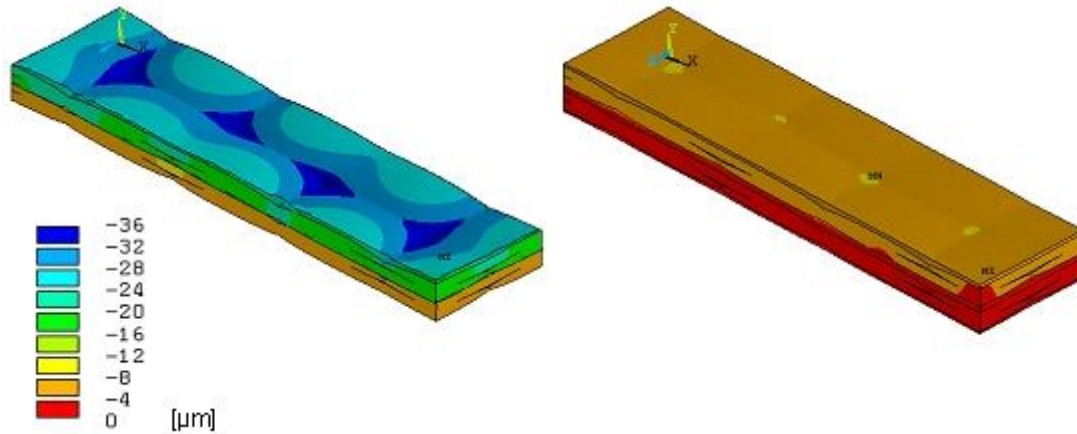


**Figure 2:** Surface waviness of semi-crystalline (left) and amorphous matrices

Another model was set up by Schubel, Warrior, and Rudd, who concentrated on the influence of different roving sizes (3 k, 6 k, and 12 k) in thermoset fiber-reinforced composites. Additionally they simulated and experimented with two matrix resins with varying CTE [5]. However, current literature showed some simplifications in the areas of heat flow, pressure application, and material models, which prevent precise predictions and, therefore, were integrated into the model developed in this work.

## 2 Development of unit cell model

The geometrical model of the organic sheet materials was created using the TexGen open-source software and LS Pre-Post from LSTC [6, 7]. The reinforcement is modeled as a twill 2/2 fabric while the matrix is polycarbonate (Fig. 3). The numerical process simulation is done using LS Dyna<sup>®</sup> from LSTC.

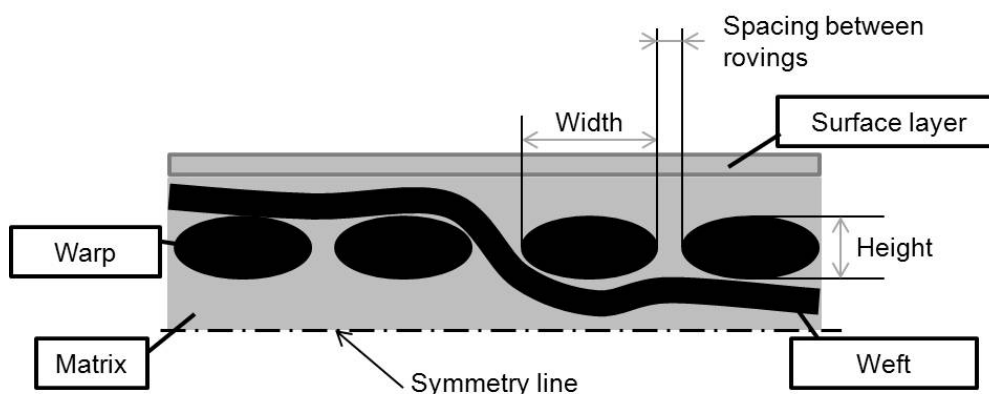


**Figure 3:** Model scheme of twill 2/2 fabric with surface layer

The unit cell was set up using the exact geometrical data from several organic sheets with the desired twill 2/2 fabric structure. The roving widths, roving heights, and the spacing between two rovings were measured from 24 samples made of polycarbonate (Makrolon 2408) and Hexcel HexForce 1102 fabric (Fig. 4). The mean values are given in Table 1.

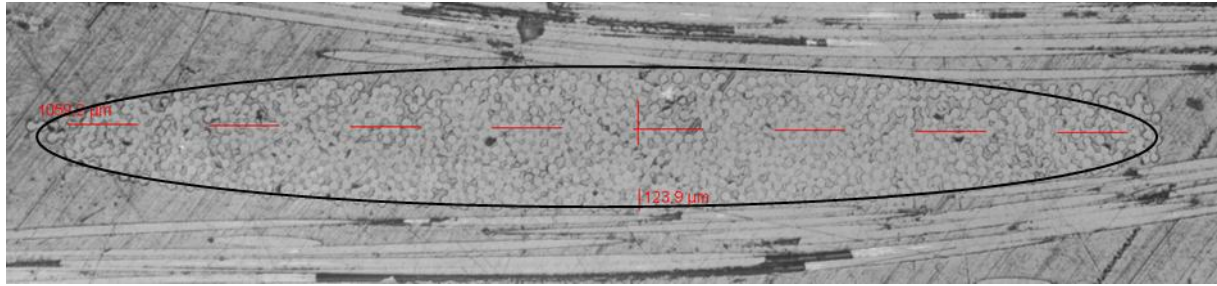


**Figure 4:** Light microscopy image of a roving in a consolidated laminate made of twill 2/2 glass fiber fabric and a polycarbonate matrix

Roving width [μm]	Roving height [μm]	Spacing between rovings [μm]
1059 ± 53	122 ± 6	316 ± 61

**Table 1:** Fabric dimensions obtained from light microscopy images

The created reinforcement structure of the unit cell is modeled with the use of hexahedral solid elements (element form 2), where each roving is created as one separate part (Fig. 5).

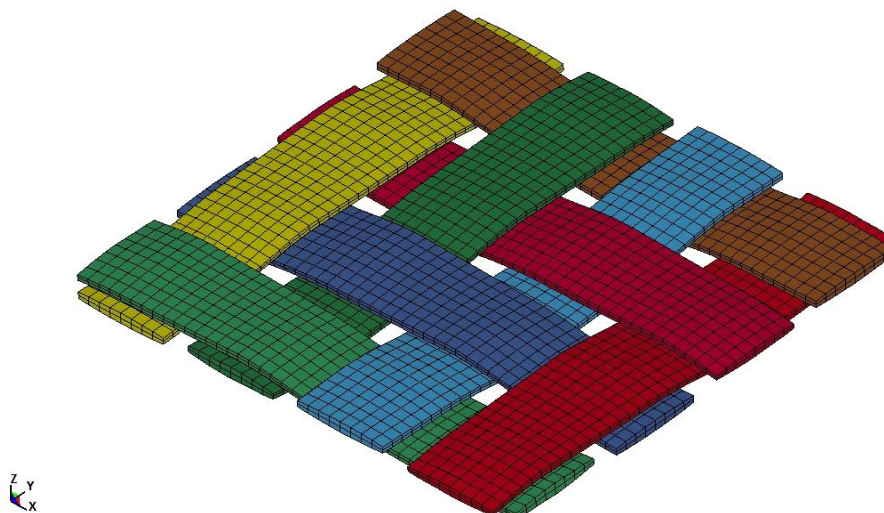


**Figure 5:** Reinforcement structure of the unit cell model

The next steps were to create the matrix around the rovings and the surface layer, which has the same properties as the matrix and is fully interconnected with the matrix network. The tool was created as a steel plate, which is needed to apply the process pressure in the thermoforming simulation (Fig. 6). As the unit cell is mirror-symmetric to the base plane the creation of one surface layer and press plate is sufficient.

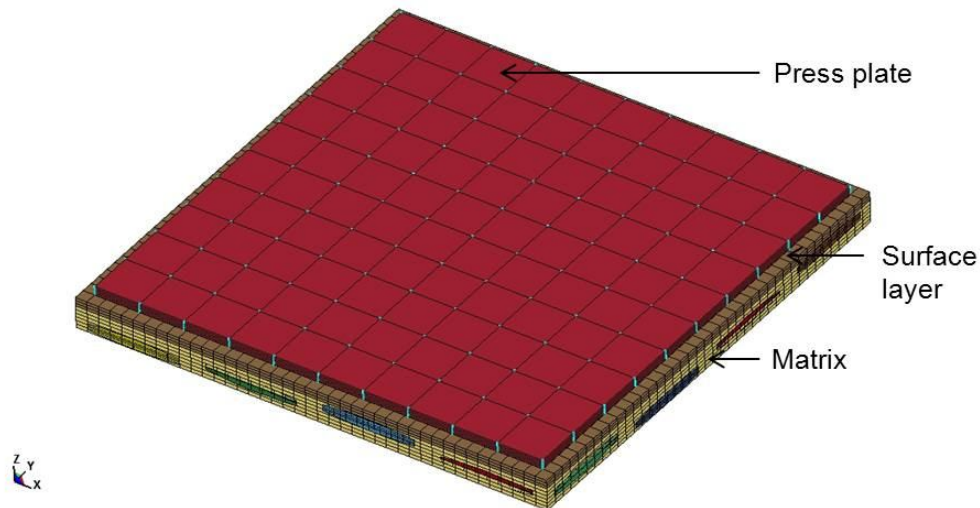


**Figure 6:** Complete unit cell model with twill 2/2 fabric, matrix, surface layer and press plate

Between the single rovings a thermal-mechanical interaction is set with the contact model “nodes to surface”, where a slave and a master segment have to be defined, and the option “thermal friction”, which enables contact conductance between rovings. Each slave node is checked for penetration through the master segment. When a penetration is detected, contact forces are calculated and applied to separate the parts. The contact between rovings and matrix is done using the constraint “Lagrange in solid”. It connects the surface nodes of the rovings with surrounding nodes of the matrix and allows compression, tension, as well as heat transfer between the bonded elements. The press plate and the surface layer with the contact model “one way surface to surface”, which enables the load transfer and thermal conductance between surface layer and press plate.

After setting the contact definitions the material models were created. The matrix and surface layer have an elastic-plastic thermal model [9, 10]. The Young’s modulus, shear modulus, and coefficient of thermal expansion are temperature dependent.

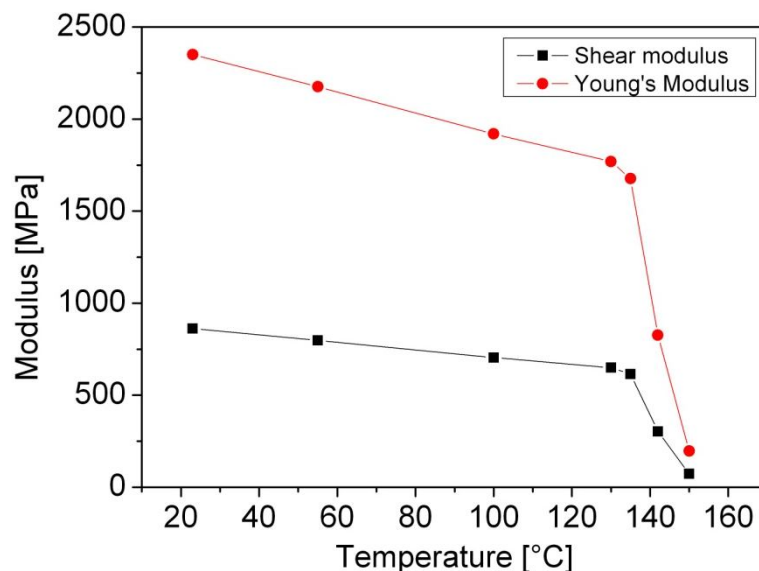


**Figure 7:** Temperature dependent Young's modulus, shear modulus for the polycarbonate matrix

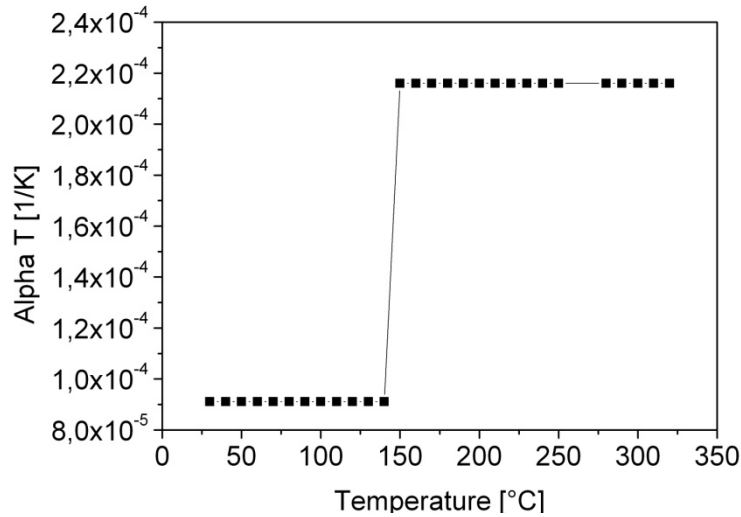


**Figure 8:** Temperature dependency for the coefficient of thermal expansion of polycarbonate

The CTE was calculated from data supplied by Bayer MaterialScience AG using equation 1.

$$\alpha^T = \frac{\Delta v_s}{v_s \cdot \Delta T} \quad (1)$$

where  $\alpha^T$  is the coefficient of thermal expansion,  $v_s$  is the specific volume,  $\Delta v_s$  is the difference in the specific volume, and  $\Delta T$  is the temperature difference.

As the rovings were simulated as solid elements the properties have to be adjusted according to the volume content  $V_f$  of 75 %. Furthermore, the rovings are modeled with an orthotropic, thermal material model, where thermal implies a temperature adaptive CTE. The orthotropic properties are oriented at a local coordinate system where  $E_A$  is in fiber direction and  $E_B$  and  $E_C$  are perpendicular to the roving direction (see equation 2 and 3). It is assumed that all filaments are parallel to each other. With the Young's modulus of the matrix  $E_M$  and the Young's modulus of the filament  $E_F$  the Young's modulus of the roving can be calculated using the linear rule of mixture.

$$E_A = \varphi \cdot E_F + (1 - \varphi) \cdot E_M \quad (2)$$

$$E_B = E_C = \frac{E_M' \cdot (1 + 0,85 \cdot \varphi^2)}{(1 - \varphi)^{1,25} + \varphi \cdot \frac{E_M'}{E_F}} \quad (3)$$

with:

$$E_M' = \frac{E_M}{1 - \nu_M^2} \quad (4)$$

where  $E_F$  is the Young's Modulus of the filament,  $E_M$  is the Young's modulus of the matrix,  $\varphi$  is the fiber volume content and  $\nu_M$  is the Poisson's ratio of the Matrix.

The thermal properties are defined in a separate material model and were assumed to be isotropic and are similar to the aforementioned matrix model.

The boundary conditions are set as follows. Due to the mirror symmetry movements of the bottom side in z-direction are restricted. To prevent tensions due to the isotropic shrinkage the side planes are not fixed, as in reality shrinkage occurs in all directions. The movement restraint between roving and matrix is defined within the "Lagrange in solid" constraint. As the press plate is just for applying the pressure the movement is restricted in z-direction. As in reality the pressure is applied over a period of time.

The unit cell's surface waviness is analyzed along the diagonal black line showed in Figure 7, as this path leads to maximum surface waviness. The characteristic waviness values were calculated according to DIN EN ISO 4287 [11].

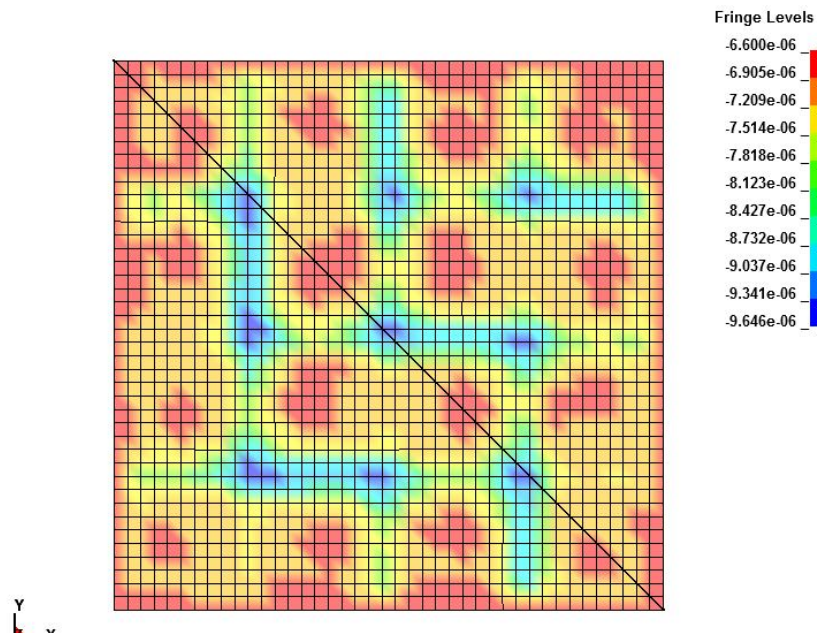


**Figure 9:** Z-displacement plot of the unit cell surface. The black diagonal line is used to calculate the characteristic waviness values

Figure 8 shows a waviness plot along the diagonal of the unit cell surface.

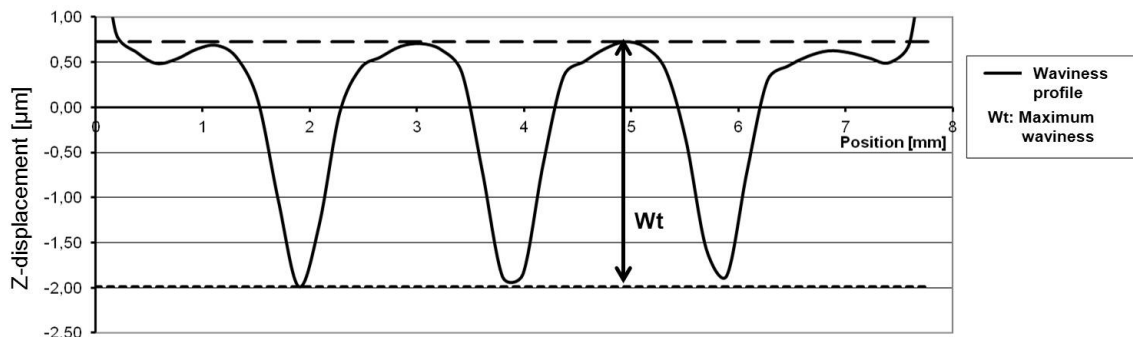


**Figure 10:** Waviness plot along the diagonal of the unit cell surface

### 3Results

#### 3.1 Influence of varying surface layer thickness

To evaluate the influence of a varying surface layer thickness several simulations with varying layer thicknesses (see table 2) were performed.

Start temperature $T_0$ [°C]	End temperature $T_{end}$ [°C]	Pressure $p$ [MPa]	Surface layer thickness $t_1$ [µm]
180	130	1	0, 50, 100, 200, 300

**Table 2:** Process parameters temperature, pressure, and surface layer thicknesses

The simulation showed a decreasing maximum waviness with increasing surface layer thickness (Fig. 9), where an increasing layer thickness acts as a cover for the fiber print-through, which is also known for thermoset systems [12]. A 200 µm surface layer decreased the waviness around 2 µm.

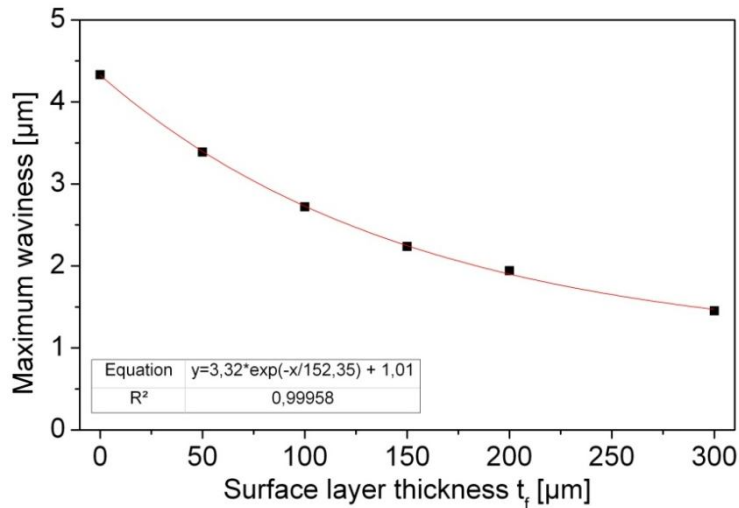


Figure 11: Influence of surface layer thickness on maximum waviness

### 3.3 Influence of nesting with 2 unit cells

In reality often more than one reinforcement layer is used and nesting becomes an issue. To investigate the effect of various unit cell displacements two configurations were simulated. Configuration one is set up with an offset just in x-direction and the second configuration with a planar offset in x- and y-direction (Fig. 12).

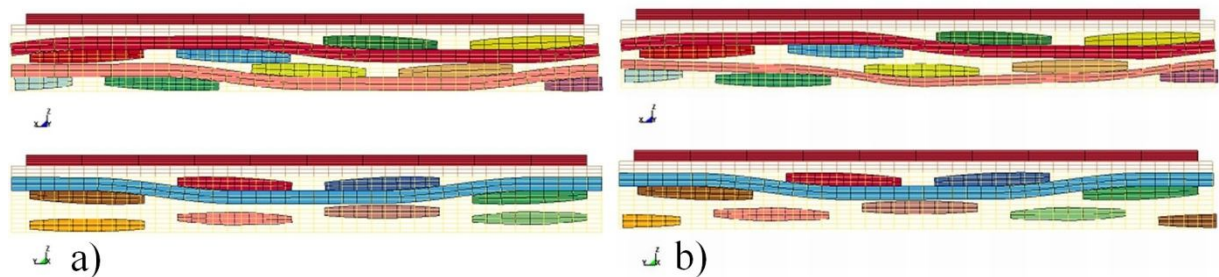


Figure 12: Offset of unit cell in a) x-direction and b) x- and y-direction

It was found that a displacement leads to a decreased maximum waviness. The effect is stronger with an offset in both directions. This is due to the decreased depth of the matrix rich regions (compare Fig. 1) as the underlying rovings decrease the free volume of matrix and therefore reduce the overall shrinkage.

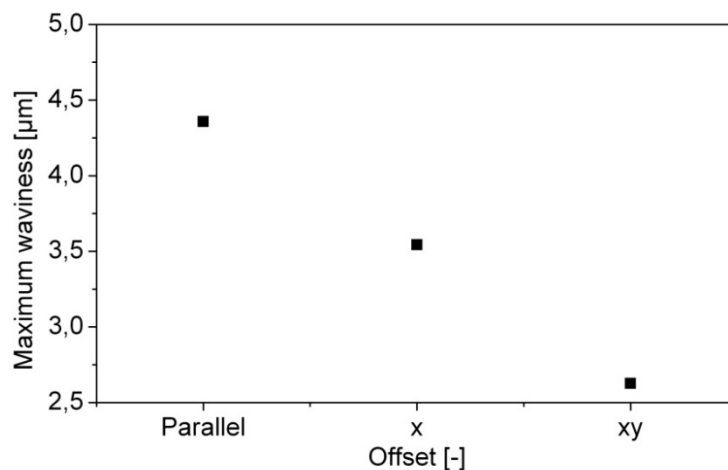


Figure 13: Maximum waviness with varying unit cell alignments

#### 4 Summary

A unit cell model to simulate the surface quality of continuous fiber-reinforced thermoplastic composites during the thermoforming process was developed. It is based on a twill 2/2 fabric structure and comprises an elastic-plastic-thermal material model for the matrix and an orthotropic mechanical, thermal model for the reinforcing fabric. The geometry data were generated from composite cross-sections using light microscopy. It includes a thickness-adaptable surface layer to investigate the effect of matrix rich surface areas on surface waviness. A thickening matrix layer was found to lower the waviness. To investigate nesting effects various displacement configurations were simulated by shifting the fabric layer below the surface layer in x and x-y direction. The displacement simulations showed a positive effect in decreasing the maximum waviness. The simulation showed that the effect of non-influenceable layer displacement can be as big as the application of surface layers and has to be considered in a possible part design.

#### 5 Acknowledgements

The research leading to these results was funded by the German Federal Ministry of Research and Development within the framework concept "WING" under grant agreement 03X0050E and supported by all the companies involved in the project.

#### References

- [1] Klein, B. *Leichtbau-Konstruktion*. Vieweg+Teubner, Wiesbaden (2009).
- [2] Ehrenstein, G. W. *Polymer Werkstoffe. Struktur – Eigenschaften - Anwendung*. Carl Hanser Verlag, München (2011).
- [3] Ostgathe, M. *Zur Serienfertigung gewebeverstärkter Halbzeuge für die Umformung*. VDI Verlag, Düsseldorf (1997).
- [4] Blinzler, M. *Werkstoff- und prozesseitige Einflussmöglichkeiten zur Optimierung der Oberflächenqualität endlosfaserverstärkter thermoplastischer Kunststoffe*. Institut für Verbundwerkstoffe GmbH, Kaiserslautern (2002).
- [5] Schubel, P. J., Warrior, N. A., Rudd, C. D. *Surface roughness Modelling of textile Composites using TexGen*. in *Proceeding of 8th international Conference on Textile Composites (Texcomp-8)*, Nottingham, UK, (2006).
- [6] Anon., TexGen. Main Page. [http://texgen.sourceforge.net/index.php/Main\\_Page](http://texgen.sourceforge.net/index.php/Main_Page) (07.11.2011).
- [7] DYNAmore, Finite Element Solutions. Software, LS-Prepost, [http://www.dynamore.de/software/ls-prepost\\_de](http://www.dynamore.de/software/ls-prepost_de) (06.11.2011).
- [8] DYNAmore Finite Element Solutions. Software. LS-Dyna, <http://www.dynamore.de/software/ls-dyna-de> (06.11.2011).
- [9] Data bank Campus 5.2. [www.CAMPUSplastics.com](http://www.CAMPUSplastics.com) (2009).
- [10] ISO data sheet, Makrolon 2408. Bayer Material Science (26.07.2010).
- [11] DIN EN ISO 4287. Geometrische Produktspezifikation (GPS) – Oberflächenbeschaffenheit: Tastschnittverfahren – Benennungen, Definitionen und Kenngrößen der Oberflächenbeschaffenheit (2010).
- [12] Massarello, J. J., Welsh, J. S., Hochhalter, J. D., Maji, A. K., Fuierer, P. A. Fiber print-through mitigation technique for composite mirror replication, *Optical Engineering*, Vol 45, pp. 123401-1-123401-8 (2006).